Ab initio pseudopotential calculations for the electronic structure of low-T_c $LuNi_2B_2C$ and the related compound LuNiBC

Hanchul Kim, Chi-Duck Hwang, and Jisoon Ihm
Department of Physics and Center for Theoretical Physics, Seoul National University, Seoul 151-742, Korea
(Received 13 December 1994; revised manuscript received 28 February 1995)

Ab initio pseudopotential calculations are performed for the electronic structure of the low-T_c intermetallics $LuNi_2B_2C$ and the related nonsuperconducting compound LuNiBC. Electronic structures of the two compounds are compared in great detail, especially in terms of the Fermi surfaces and the symmetry-decomposed density of states (DOS) near the Fermi level. The estimated electron-phonon coupling constant λ (0.8–1.1) from the heat-capacity data as well as from the calculated DOS at E_F indicates that T_c of $LuNi_2B_2C$ is reasonably well explained by the conventional Bardeen-Cooper-Schrieffer mechanism with intermediate coupling strength. The relatively high T_c arises from the large DOS at the Fermi level. Absence of superconductivity in LuNiBC may be understood to be due to the reduced DOS at E_F. Unlike the high-T_c cuprates, the low-T_c $LuNi_2B_2C$ does not have the half-filled σ-antibonding bands and its electronic structure is almost three dimensional despite the layered atomic structure.

I. INTRODUCTION

Recently Cava *et al.*[1] investigated superconductivity in the Ni-based quaternary intermetallics LNi_2B_2C with L = Y, La, Ce, Sm, Tb, Dy, Ho, Er, Tm, and Lu. Superconductivity was found not only in the nonmagnetic Y and Lu but also in the magnetic rare-earth Tm, Er, and Ho compounds. For other magnetic rare earths, LNi_2B_2C compounds were not superconducting down to 4.2 K. The highest T_c among the single-phase crystals has been realized in $LuNi_2B_2C$ with T_c = 16.6 K. Siegrist *et al.*[2] have observed that this superconducting compound is a member of a homologous series of compounds of general formula $(LuC)_m(NiB)_n$, where the $m = 1$, $n = 2$ member is the 16.6 K superconductor and the $m = n = 2$ member is nonsuperconducting. This series exhibits a layered atomic structure, reminiscent of the high-T_c cuprates. The superconducting compound $LuNi_2B_2C$ crystallizes in the body-centered tetragonal (bct) structure and its space group is $I4/mmm$. The LuC (NaCl-type) layers alternate with $(NiB)_2$ layers in a stoichiometry of 1:1. The $(NiB)_2$ layers contain a square-planar Ni_2 array sandwiched between the boron planes with nickel atoms being tetrahedrally coordinated to four boron atoms. The Ni-Ni in-plane distance is 2.45 Å, which is shorter than that found in the metallic nickel (2.50 Å). This suggests strong Ni-Ni metallic bonding. The atomic structure of LuNiBC is formed by substituting the rocksalt-type $(LuC)_2$ bilayer for the LuC monolayer in $LuNi_2B_2C$ and the Bravais lattice is changed from bct to simple tetragonal (st) and the resulting space group is nonsymmorphic $P4/nmm$.

On the theoretical side, three works[3–5] based on the linear augmented-plane-wave method and one[6] using the augmented-spherical-wave method have been published recently. They all indicate that $LuNi_2B_2C$ is a three-dimensional metal belonging to the family of conventional superconductors. Mattheiss[3] has presented the electronic structures of $LuNi_2B_2C$, LuNiBC, and YNi_2B_2C and pointed out that these borocarbides do not satisfy the *ad hoc* band criteria for identifying potential high-T_c candidates.[7] Pickett and Singh[4] have deduced a strong electron-phonon coupling constant $\lambda \sim 2.6$ from resistivity data and calculated the frequency ($\sim$ 106 meV) of the boron a_{1g} phonon mode. They have suggested that superconductivity in $LuNi_2B_2C$ may involve either soft modes or phonon contributions from heavier atoms. Mattheiss *et al.*[5] have suggested that the high-frequency B a_{1g} phonon mode (B-C stretching mode in nature) and its strong coupling to the s-p band near E_F are essential to superconductivity in $LuNi_2B_2C$. Coehoorn[6] has analyzed the character of the states in the energy range of -0.2 to 0.2 eV with respect to the Fermi level. In the present work, we intend to provide more detailed information on the electronic structure, i.e., mapping of the whole Fermi surface (FS), and a thorough investigation of the character of the Fermi-level states via the charge-density plots and the analysis of partial density of states near E_F, and to determine unambiguously essential ingredients to the relatively high T_c in this family of quaternary intermetallic borocarbides. In doing so, we hope to establish that the *ab initio* pseudopotential method with the plane-wave basis set is at least as competitive as other methods[3–6] for the electronic structure calculation of complex materials.

II. COMPUTATIONAL METHOD

We make a comparative study of the electronic structures of $LuNi_2B_2C$ and LuNiBC by means of the *ab initio* pseudopotential plane-wave calculation[8] within local-

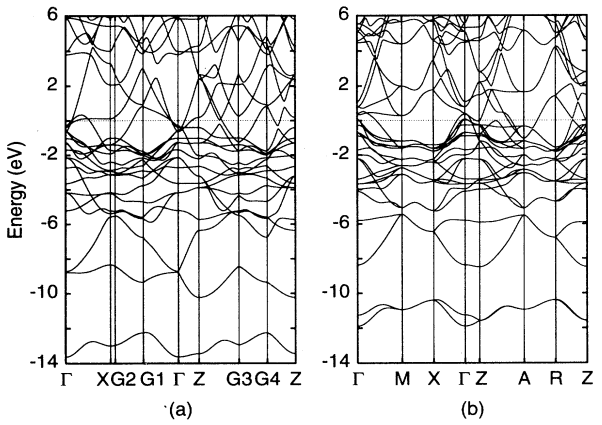

FIG. 1. Energy band structures of (a) $LuNi_2B_2C$ and (b) LuNiBC. The labeled symmetric points defined in terms of Cartesian coordinates are as follows: in (a), $X = (\frac{\pi}{a}, \frac{\pi}{a}, 0)$, $G1 = (\eta, 0, 0)$, $G2 = (\eta, \zeta, 0)$, $G3 = (\zeta, \zeta, \frac{2\pi}{c})$, $G4 = (\zeta, 0, \frac{2\pi}{c})$, and $Z = (0, 0, \frac{2\pi}{c})$ [where $\eta \equiv \frac{\pi}{a}(1 + \frac{a^2}{c^2})$ and $\zeta \equiv \frac{\pi}{a}(1 - \frac{a^2}{c^2})$], and in (b), $M = (\frac{\pi}{a}, \frac{\pi}{a}, 0)$, $X = (\frac{\pi}{a}, 0, 0)$, $Z = (0, 0, \frac{\pi}{c})$. $A = (\frac{\pi}{a}, \frac{\pi}{a}, \frac{\pi}{c})$, and $R = (\frac{\pi}{a}, 0, \frac{\pi}{c})$.

density-functional theory.[9] Soft norm-conserving pseudopotentials are generated nonrelativistically following the scheme of Troullier and Martins[10] and cast into the fully nonlocal form of Kleinman and Bylander.[11] The exchange-correlation potential is included via the Perdew-Zunger parametrization of the Ceperley-Alder functional.[12] An energy cutoff of 72.25 Ry, which results in about 4500 and 6600 plane waves in the basis set for $LuNi_2B_2C$ and LuNiBC, respectively, is used and found to yield 1 meV accuracy in the Fermi energy. The diagonalization of the Hamiltonian matrices is achieved through the iterative method of Davidson and Liu[13] with the modified Jacobi relaxation. The Brillouin zone (BZ) integration is performed with the use of as many as 415 and 275 linear tetrahedral **k** points in the irreducible Brillouin zone (IBZ, 1/16 of BZ) for $LuNi_2B_2C$ and LuNiBC, respectively. The structural parameters obtained from experiment[2,14] are used in the calculation.

III. RESULTS

A. $LuNi_2B_2C$

The calculated energy band structure of $LuNi_2B_2C$ is presented in Fig. 1(a). The C($2s$) band lies in the energy range between -14 and -12 eV. The B($2s$)-C($2p$) hybridized bands extend from -10 to -8.5 eV. The main valence band complex is composed of contributions from all atoms in the compound. Near E_F, these bands exhibit an appreciable dispersion along the c-axis direction, indicating that this compound is a three-dimensional metal in spite of the apparent two dimensionality in its atomic structure. This result is consistent with other calculations.[3–6] The three bands crossing E_F produce five electronic FS's: two prolate spheroids centered at Γ with their long axes parallel to the c axis, two square-planar pancakes centered at P with sides parallel to (100) and (010) directions as shown in Fig. 2(a), and the most complex one whose main portion is a cylindrical surface (parallel to the c axis and centered at X, a reflection of the two-dimensional nature of the atomic structure) constricted along (100) and (010) directions near the $k_z = \pi/c$ plane as shown in Fig. 2(b). The topology of the FS's is not changed when the Fermi energy varies within the computational accuracy (1 meV). One spheroid at Γ originates from the Lu($d_{x^2-y^2}$) subband and exhibits a $dd\sigma$-bonding character with some admixture of the C($p_{x,y}$) character. The other spheroid at Γ has the character of Ni($d_{x^2-y^2}$)-B(p_z)-C(p_z) hybridization with contributions from the near-neighbor Ni($d_{yz\pm zx}$) hybridized orbitals and Lu($d_{yz,zx}$, $d_{3z^2-r^2}$) orbitals. A pair of square-planar pancakes is related to the flat band just above E_F along the Γ-X direction and has the character of Ni(d_{xy}) $dd\sigma^\star$ ($\star$ indicates antibonding), which originates from the strong metallic hybridization between near-neighbor Ni atoms, with Ni($d_{3z^2-r^2}$)-B($p_{x,y}$)-Lu($d_{yz,zx}$) hybridization. The main character of the constricted cylinder is the same as that of the second spheroid. The remaining portion attached to the constricted cylinder has the same character as that of the square-planar pancakes.

A pair of contour plots of the symmetrized probability amplitude $|\psi_{nk}(\boldsymbol{r})|^2$ is presented in Fig. 3 to illus-

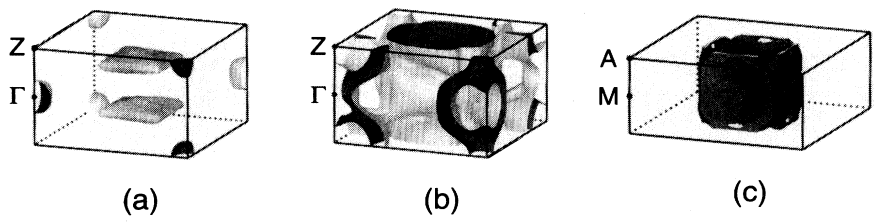

FIG. 2. Overview of (a) the two square-planar pancakelike FS's and one-electron spheroidal FS at Γ of $LuNi_2B_2C$, (b) the most complex constricted cylindrical FS of $LuNi_2B_2C$, and (c) the main hole FS of LuNiBC. The bounding box has the same volume as the first Brillouin zone. The box centers are the X point in (a) and (b) and the Γ point in (c), respectively. The darker side of the Fermi surface indicates the low-energy direction where electronic states are occupied.

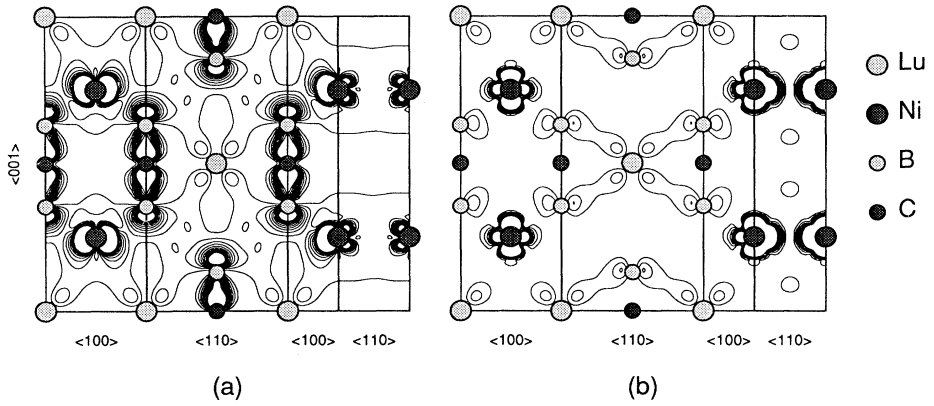

FIG. 3. Contour plots of the symmetrized probability amplitude for $LuNi_2B_2C$. (a) The 21st band and (b) the 22nd band at the **k** point $\frac{0.56\pi}{a}$ (1, 1, 0). Contour values run from 0.002 to 0.02 in steps of 0.002 electrons/unit cell.

trate the characteristic electronic states near E_F in this compound. In Fig. 3(a), the Ni($d_{x^2-y^2}$)-B(p_z)-C(p_z) hybridization, the near-neighbor Ni($d_{yz\pm zx}$) hybridized orbitals, and Lu($d_{yz,zx}$) orbitals are clearly shown. Those are the characteristic charge distributions on the constricted cylindrical FS. Shown in Fig. 3(b) are the Ni(d_{xy}) $dd\sigma^\star$ hybridization and the Ni($d_{3z^2-r^2}$)-B($p_{x,y}$)-Lu($d_{yz,zx}$) hybridization which are the characteristics of the states on the square-planar pancakes.

The total density of states (TDOS) and the local (*or* site-projected) density of states (LDOS) are shown in Fig. 4(a). (The radii of the spherical volume used to calculate the LDOS are 2.60, 1.83, 1.38, and 1.40 a.u. for Lu, Ni, B, and C, respectively.) The Fermi level lies just below a DOS peak. The TDOS at E_F [$N(E_F)$] is 3.88 states/(eV unit cell) and the resulting DOS per Ni atom [1.94 states/(eV Ni)] is larger than 1.41 states/(eV Cu) for $YBa_2Cu_3O_7$.[15] [A somewhat larger $N(E_F)$ ($\approx$ 4.8) reported in Refs. 3 and 4 is presumably due to their use of a relativistic scheme.] Under the assumption of the rigid band, an additional 0.43 electron per unit cell would shift the Fermi level to the DOS peak (located 0.094 eV above the present Fermi level) with $N(E_F) \simeq 4.83$ states/(eV unit cell). The Ni(3*d*) DOS peak around E_F is separated from the main body of the Ni(3*d*) DOS by $\sim$ 1 eV. The LDOS at E_F are 0.33, 0.94, 0.12, and 0.14 states/(eV atom) for Lu, Ni, B, and C, respectively, which shows that all atoms more or less contribute to the states near E_F with the dominant contributions from Ni. The partial (*or* site-projected and symmetry-decomposed) density of states (PDOS) is shown in Fig. 4(b) in an expanded scale and clearly exhibits both Ni(d_{xy}, $d_{3z^2-r^2}$)-Lu($d_{yz,zx}$)-B($p_{x,y}$) hybridization and Ni($d_{x^2-y^2}$, $d_{yz,zx}$)-Lu($d_{yz,zx}$, $d_{3z^2-r^2}$)-B(p_z)-C(p_z) hybridization near E_F. These hybridized states near E_F are not confined to two-dimensional atomic layers and the electronic properties of this material are truly *three* dimensional. Coehoorn[6] has extracted the same conclusion via the analysis of the PDOS integrated in the interval from -0.2 to 0.2 eV with respect to E_F. The partial charge of Ni(3*d*) within the spherical volume of radius $1.83a_B$ is 7.7 electrons/Ni which is smaller than that of Cu(3*d*) in high-T_c cuprates (typically $\sim$ 8.6 electrons/Cu).[15]

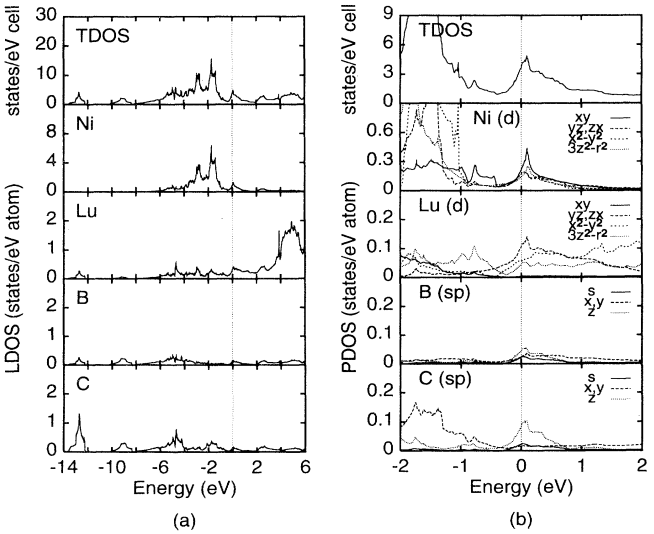

FIG. 4. (a) TDOS and LDOS, (b) TDOS and PDOS of $LuNi_2B_2C$ in an expanded scale. Note that vertical scales vary among figures.

B. LuNiBC

The calculated energy band structure of LuNiBC is shown in Fig. 1(b). An interesting feature here is that all the bands are doubly degenerate on the BZ boundaries whose normal vectors are perpendicular to the *c*-axis direction. Nonsymmorphic operations in the space group are responsible for this degeneracy. A pair of C($2s$) bands lie between -12 and -10.5 eV and B($2s$)-C($2p$) hybridized bands range from -8.5 to -6.5 eV. The main valence band complex is formed by the contributions from all atoms as in $LuNi_2B_2C$. Near the Fermi level, the energy bands are dispersive along the *c*-axis direction, suggesting three-dimensional electronic properties as in $LuNi_2B_2C$. We find five bands crossing E_F. These five bands produce six FS's: a pair of hole pockets at Γ, one large hole FS centered at Γ, two electron pockets at A, and one tiny needlelike electron pocket at Z. The two hole pockets at Γ have the character of Ni($d_{yz,zx}$)-C($p_{x,y}$) with small contributions from Lu($d_{x^2-y^2}$) and B($p_{x,y}$). The character of

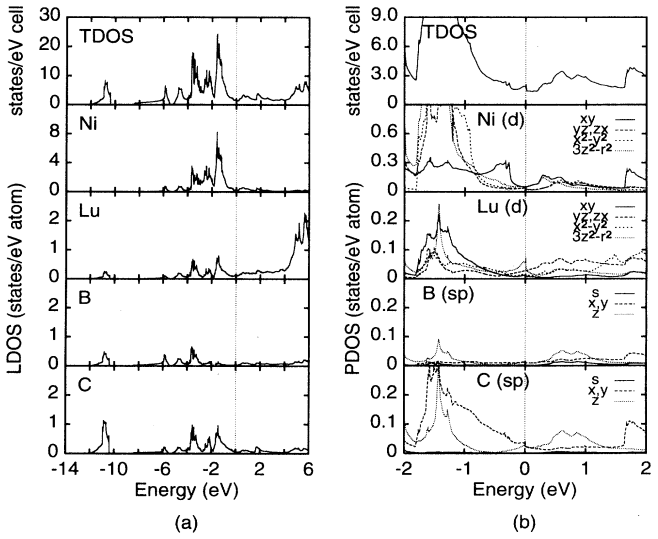

FIG. 5. (a) TDOS and LDOS, (b) TDOS and PDOS of LuNiBC in an expanded scale. Note that vertical scales vary among figures.

the large hole FS (which is the main FS of this non-superconducting compound) shown in Fig. 2(c) is rather complex and Lu($d_{3d^2-r^2}$)-Ni($d_{yz,zx}$, $d_{x^2-y^2}$)-B($2p$)-C($2p$) hybridization prevails with some contributions from the other Lu($5d$) subbands and the Ni(d_{xy}) subband. Judging from the topology of the large hole FS, LuNiBC is more three dimensional in its electronic properties than $LuNi_2B_2C$. The two electron pockets at A have the character of Lu($d_{yz,zx}$)-Ni(d_{xy}, $d_{3z^2-r^2}$)-B($2p$)-C($2p$).

The TDOS and the LDOS are shown in Fig. 5(a). The Fermi level of LuNiBC lies at a valley of the TDOS in contrast to the case of $LuNi_2B_2C$, resulting in a much reduced $N(E_F)$ [= 1.95 states/(eV unit cell)] compared with 3.88 for the superconducting $LuNi_2B_2C$. One notable feature is that the isolated peak of the LDOS for Ni above E_F separated from the main one below E_F is much broader than the corresponding peak in $LuNi_2B_2C$. More details can be obtained from the PDOS in Fig. 5(b) drawn in an expanded scale near E_F. Unlike in $LuNi_2B_2C$, the peaks of the five Ni($3d$) PDOS above E_F do not all coincide. The Ni(d_{xy}) subband and the Ni($d_{3z^2-r^2}$) subband produce a coincident peak in the PDOS at 0.3 eV above E_F with some hybridization with Lu($d_{yz,zx}$) subbands, and this peak is related to the flat band along the Γ-M direction above E_F. The other three Ni($3d$) subbands hybridize with B($2p$), C(p_z), and Lu($5d$) subbands to form a pair of broad peaks at 0.6 and 0.9 eV. The high-energy peak reflects Ni($d_{x^2-y^2}$)-B(p_z)-C(p_z) hybridization with some additional contributions from Ni($d_{yz,zx}$) and Lu($d_{3z^2-r^2}$) states. The low-energy peak has the character of Lu($d_{yz,zx}$)-Ni($d_{x^2-y^2}$, d_{xy}, $d_{yz,zx}$)-B(p_z)-C(p_z) hybridization. The flat band along Γ-Z-A manifests itself as a peak at -0.3 eV in the Ni(d_{xy}) PDOS. Another tiny peak of Lu($d_{3z^2-r^2}$)-C($p_{x,y}$) character found at E_F is related to the flat part (encountered along Z-R) of the large hole FS.

IV. DISCUSSION

The overall feature of the electronic structure of these Lu-Ni-B-C compounds indicates that these compounds are three-dimensional metals and we will argue that superconductivity observed in $LuNi_2B_2C$ should be based on the conventional mechanism rather than an exotic one. Our conclusion agrees with other theoretical works, although details are somewhat different as described below. Recently Carter *et al.*[16] reported heat capacity measurements on $LuNi_2B_2C$ and found that fitting to the low-temperature form $\gamma T + \beta T^3$ yields $\gamma \simeq 19$ mJ/mol K^2 and $\beta \simeq 2.67 \times 10^{-4}$ J/mol K^4. Incorporating the Debye model for the phonon dispersion, the effective Debye temperature Θ_D is estimated to be 345 K (≈ 30 meV). The electron-phonon coupling constant λ can be estimated using the relation $\gamma = (1+\lambda)\gamma_{\rm band}$. The band-structure value of the Sommerfeld parameter $\gamma_{\rm band}$ defined by $\frac{\pi^2}{3}k_B^2 N(E_F)$ is 9.15 mJ/mol K^2 and the estimated λ is 1.08. Or, with the observed T_c of 16.6 K, the estimated Debye temperature, and the calculated DOS at E_F, we can estimate λ backwards using one of the following T_c equations:

$$k_B T_c = 1.13\,\hbar\omega_{\rm ph}\exp\left\{-\frac{1+\lambda}{\lambda-\mu^*(1+\lambda)}\right\} \quad (1)$$

and

$$k_B T_c = \frac{\omega_{\log}}{1.2}\exp\left\{-\frac{1.04(1+\lambda)}{\lambda-\mu^*(1+0.62\lambda)}\right\}, \quad (2)$$

where $\omega_{\log}$ is chosen to be $0.7\omega_{\rm ph}$ and $\omega_{\rm ph}$ is regarded to be the same as $\omega_D \equiv k_B\Theta_D/\hbar$. Assuming the Coulomb pseudopotential $\mu^* = 0.13$, the estimated λ's are 0.80 and 1.08 using the renormalized Bardeen-Cooper-Schrieffer (BCS) formula [Eq. (1)] and the McMillan formula [Eq. (2)], respectively. The electron-phonon coupling constant in the range of 0.8–1.1 indicates that $LuNi_2B_2C$ is a conventional superconductor with intermediate coupling strength in which the relatively high T_c results from the large value of the DOS at the Fermi level contributed by Ni d electrons (but not too large to induce ferromagnetic instability). According to our analysis on λ, very strong coupling $\lambda \sim 2.6$ obtained and discussed in Ref. 4 (which would lead to unreasonably overestimated T_c) is not necessary. The strong coupling of the high-frequency B a_{1g} phonon mode to the s-p band near E_F emphasized in Ref. 5 does not seem to be essential either, though it does give some contributions to the superconductivity in $LuNi_2B_2C$, because the LDOS at E_F indicates that contributions from B and C to $N(E_F)$ are much less than that from Ni. In other words, a large $N(E_F)$ contributed mainly from Ni and the moderately strong electron-phonon coupling together account for $T_c \sim 17$ K. Under the assumption that λ is proportional to $N(E_F)$, we can make a crude estimate of the T_c of the related compound LuNiBC. The resulting T_c falls in the range 0.7–2.6 K with use of the two T_c equations mentioned above. Such a dramatic reduction of T_c by taking into account the change in $N(E_F)$ alone is con-

sistent with the absence of superconductivity in LuNiBC down to the liquid helium temperature and supports the BCS mechanism for the superconductivity in this family of materials.[17] Enhancing T_c further by optimizing material variables here seems quite limited within the rigid-band picture since the Fermi level of $LuNi_2B_2C$ already lies close to the local peak of the DOS. If we could shift the Fermi level to the position of the DOS peak where $N(E_F)$ is 4.83 compared with 3.88 states/(eV unit cell) in real $LuNi_2B_2C$, the T_c would go up to 22–26 K, not an impressive enhancement over 16.6 K. This value is also close to the highest T_c (23 K for Y-Pd-B-C) reported in this family of quaternary intermetallic borocarbides so far.

We mentioned in the Introduction that Mattheiss[7] has proposed an *ad hoc* band criterion for identifying possible high-T_c candidates: the existence of almost *half-filled* $\sigma^\star$ bands (typically due to strong nearest-neighbor hybridization between nearly degenerate cation-anion levels). The absence of $\sigma^\star$ bands here can be attributed to the weaker Ni-B bonds around the tetrahedrally coordinated Ni atoms than the Cu-O bonds in the CuO_2 planes of cuprates. This is also related to the three-dimensional electronic character of $LuNi_2B_2C$ originating from the strong interlayer interaction via bridging carbon atoms [mainly in terms of Ni($d_{x^2-y^2}$)-B(p_z)-C(p_z) hybridization] in contrast to the much weaker interlayer interaction in high-T_c cuprates resulting in quasi-two-dimensional electronic properties.

In summary, we report *ab initio* pseudopotential studies of the newly synthesized $LuNi_2B_2C$ and LuNiBC within local-density-functional theory. The band structure, TDOS, LDOS, PDOS, and FS are presented for both compounds. The presence of a much constricted cylindrical FS in $LuNi_2B_2C$ is reminiscent of the two-dimensional atomic structure of these compounds. Otherwise, the electronic structures of both materials are predominantly three dimensional. The estimate of the electron-phonon coupling constant for $LuNi_2B_2C$ from heat-capacity data as well as from theoretical considerations yields $0.8 \leq \lambda \leq 1.1$, indicating a moderately coupled conventional superconductor with the relatively high T_c resulting mainly from the large $N(E_F)$. The reduced $N(E_F)$ of LuNiBC compared with $LuNi_2B_2C$ is probably the reason for the absence of superconductivity in LuNiBC. The states near the Fermi level are dominated by the Ni(3*d*) character, still with some contributions from other atoms. Ni(3*d*) and B(2*p*) states hybridize by a noticeable amount around E_F, but the strength of such a hybridization is not so great as that of Cu-O hybridization within the CuO_2 planes in high-T_c cuprates. Bridging carbon atoms provide strong interlayer interactions which yield the three-dimensional electronic structure. Although both $LuNi_2B_2C$ and high-T_c cuprates have layered structures, $LuNi_2B_2C$ lacks in nearly half-filled $\sigma^\star$ bands which are regarded as crucial to a high T_c in cuprates.

ACKNOWLEDGMENTS

This work was supported by the Ministry of Science and Technology, the BSRI Grant No. 94-2420 of the Ministry of Education, and the Korea Science and Engineering Foundation through the SRC program.

[1] R. J. Cava, H. Takagi, H. W. Zandbergen, J. J. Krajewski, W. F. Peck, Jr., T. Siegrist, B. Batlogg, R. B. von Dover, R. J. Felder, K. Mizuhashi, J. O. Lee, H. Eisaki, and S. Uchida, Nature **367**, 252 (1994).

[2] T. Siegrist, H. W. Zandbergen, R. J. Cava, J. J. Krajewski, and W. F. Peck, Jr., Nature **367**, 254 (1994).

[3] L. F. Mattheiss, Phys. Rev. B **49**, 13 279 (1994).

[4] W. E. Pickett and D. J. Singh, Phys. Rev. Lett. **72**, 3702 (1994).

[5] L. F. Mattheiss, T. Siegrist, and R. J. Cava, Solid State Commun. **91**, 587 (1994).

[6] R. Coehoorn, Physica C **228**, 331 (1994).

[7] L. F. Mattheiss, Phys. Rev. B **47**, 8224 (1993).

[8] J. Ihm, A. Zunger, and M. L. Cohen, J. Phys. C **12**, 4409 (1979); **13**, 3095(E) (1980).

[9] P. Hohenberg and W. Kohn, Phys. Rev. **136**, B864 (1964); W. Kohn and L. J. Sham, *ibid.* **140**, A1133 (1965).

[10] N. Troullier and J. L. Martins, Phys. Rev. B **43**, 1993 (1991).

[11] L. Kleinman and D. M. Bylander, Phys. Rev. Lett. **48**, 1425 (1982).

[12] J. P. Perdew and A. Zunger, Phys. Rev. B **23**, 5048 (1981).

[13] E. R. Davidson, J. Comput. Phys. **17**, 87 (1975); B. Liu (unpublished).

[14] We have used the experimental structural parameters $a = 3.4639$ Å, $c = 10.6313$ Å, and the atomic positions Lu(0, 0, 0), Ni($a/2$, 0, $c/4$) and (0, $a/2$, $c/4$), B(0, 0, $\pm 0.3621c$), and C($a/2$, $a/2$, 0) for $LuNi_2B_2C$ and $a = 3.4985$ Å, $c = 7.7556$ Å, and the atomic positions Lu($\pm a/4$, $\pm a/4$, $\pm 0.1620c$), Ni($\pm 3a/4$, $\pm a/4$, $\pm c/2$), B($\mp a/4$, $\mp a/4$, $\pm 0.3489c$), and C($\mp a/4$, $\mp a/4$, $\pm 0.1523c$) for LuNiBC. The atomic positions of B and C of LuNiBC are interchanged, presumably by a typographical error, in Ref. 2.

[15] H. Kim and J. Ihm, Phys. Rev. B **51**, 3886 (1995).

[16] S. A. Carter, B. Batlogg, R. J. Cava, J. J. Krajewski, and W. F. Peck, Jr., Phys. Rev. B **50**, 4216 (1994).

[17] If we insist on the boron a_{1g} optical phonon mode ($\omega_{ph} \sim 106$ meV according to the estimate in Ref. 4), $\lambda \sim 0.55$–0.63 for $LuNi_2B_2C$ and $T_c \sim 0.01$–0.15 K for LuNiBC are obtained.

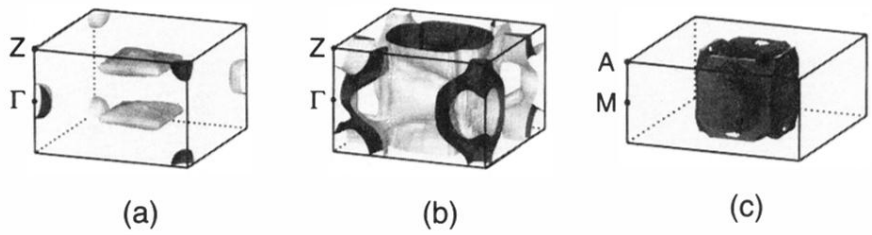

FIG. 2. Overview of (a) the two square-planar pancakelike FS's and one-electron spheroidal FS at Γ of $LuNi_2B_2C$, (b) the most complex constricted cylindrical FS of $LuNi_2B_2C$, and (c) the main hole FS of LuNiBC. The bounding box has the same volume as the first Brillouin zone. The box centers are the X point in (a) and (b) and the Γ point in (c), respectively. The darker side of the Fermi surface indicates the low-energy direction where electronic states are occupied.